A two-carrier detector: evading 3dB quantum penalty in heterodyne readout

Teng Zhang[1], Philip Jones[1], Haixing Miao[1], Denis Martynov[1], Andreas Freise[1,2,3], and Stefan W. Ballmer[4]

[1] *School of Physics and Astronomy, and Institute of Gravitational Wave Astronomy, University of Birmingham, Edgbaston, Birmingham B15 2TT, United Kingdom*

[2] *Department of Physics and Astronomy, VU Amsterdam, De Boelelaan 1081, 1081, HV, Amsterdam, The Netherlands*

[3] *Nikhef, Science Park 105, 1098, XG Amsterdam, The Netherlands and*

[4] *Syracuse University, Syracuse, NY 13244, USA*

Quantum measurements with heterodyne readout suffers 3dB fundamental quantum-noise penalty from additional vacuum compared with homodyne readout. We propose a two-carrier detector design with heterodyne readout that has an identical performance to homodyne readout. It naturally achieves low-frequency signal measurements with high-frequency two-mode quantum squeezing, which avoids the classical noise at audio frequencies. In addition, it is also compatible with other quantum nondemolition techniques.

Introduction — Since 2015, laser interferometric gravitational-wave detectors have made a series of direct observations of gravitational waves from mergers of binary black holes and neutron stars [1–3]. They have opened a new observational window into the universe and provided significant new inputs to many scientific fields. These detectors are dual-recycled Fabry–Perot Michelson interferometers. In the interferometer, a laser field is pumped from the symmetric port, enhanced in the power recycling cavity and then circulated in the two Fabry–Perot arm cavities, which senses the motion of test masses induced by the gravitational waves. This probe laser is called the carrier. When the interferometer operates at the dark fringe, the carrier will return to the symmetric port while the signal sidebands encoding the differential motion of two arm cavities enter into the anti-symmetric port. The signal-recycling cavity plays the role of circulating the signal sidebands, which shapes the frequency-dependent response of the interferometer [4, 5]. To translate the electromagnetic sidebands into a measurable electrical signal, an optical readout scheme is required, which is also fundamental for determining the sensitivity of the detector [6].

Heterodyne readout is widely implemented in precision measurements, for example, for the stabilisation of laser frequencies and optical cavities (also know as Pound-Drever-Hall technique [7–13]) and the quantum squeezing characterisation with its natural immunity to the low-frequency classical noise [14–18]. In conventional heterodyne readout, the local oscillator beats with two fields that lie symmetrically besides the local oscillator with demodulation frequency ω_m away (they are sometimes called signal and image sidebands [19]). Compared with homodyne readout, the heterodyne readout suffers from 3 dB noise penalty due to the additional image vacuum [19–22]. The additional noise penalty is a direct and necessary consequence of the Heisenberg uncertainty principle when all quadratures are allowed to be measured simultaneously [23]. In the first-generation gravitational wave detectors, *e.g.* LIGO [24], Virgo [25], TAMA [9], GEO600 [26], a heterodyne readout with two balanced radio frequency (RF) sidebands was used, the a factor of 2 (3 dB) quantum penalty got reduced to a factor of 1.5. In the subsequent detector upgrades the readout scheme was switched to DC readout [27, 28], a variant of homodyne readout. The local oscillator in the DC readout is derived by slightly detuning the arm cavities, which offsets the interferometer from the perfect dark fringe. DC readout has the advantage of a straightforward implementation without needing an external local

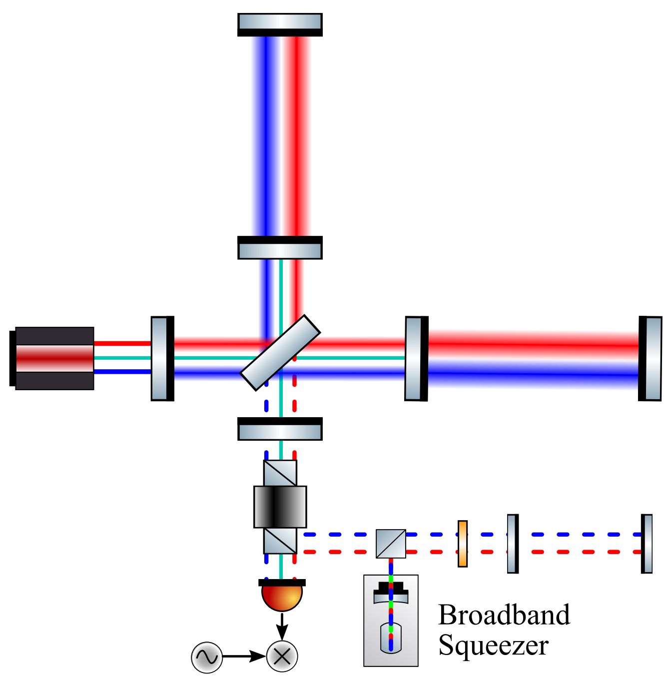

FIG. 1. Schematic of the two-carrier gravitational-wave detector with heterodyne readout. The red laser corresponds to the carrier at ω_1, the blue laser corresponds to the carrier at ω_2 and the cyan laser corresponds to the local oscillator at $\omega_L = (\omega_1 + \omega_2)/2$. The broadband squeezer has a bandwidth larger than $(\omega_2 - \omega_1)/2$, but without the need of squeezing at audio frequencies.

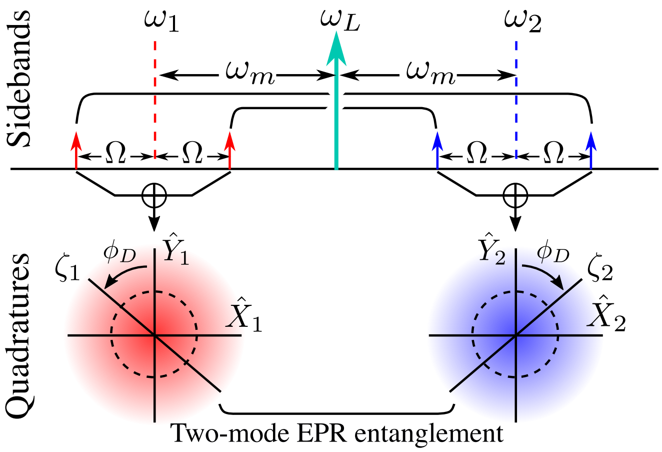

FIG. 2. Schematics of heterodyne readout with two-mode squeezing in the sidebands and the quadratures picture. The sidebands of which the sum of frequencies equals to $\omega_1 + \omega_2$ are entangled. This leads to a two-mode EPR entanglement between quadratures on ζ_1 and ζ_2 of two modes. Ω is the frequency of the audio signal sideband.

oscillator. However, the dark-fringe offset induces extra couplings of technical noises and is not ideal for future-generation gravitational wave detectors [29]. A balanced homodyne readout can eliminate the dark fringe offset by introducing spatially separated local oscillator [6]. This requires auxiliary optics on the local oscillator path and additional output optical mode cleaner, which introduces extra complexities [30]. Meanwhile, heterodyne readout is still used in the current detectors for the stabilisation of auxiliary degrees of freedom, such as the lengths of the dual recycling cavities [31, 32].

Is there a way of evading the fundamental quantum noise penalty in heterodyne readout? It was found that the noise penalty of heterodyne readout could be evaded if the image vacuum bands can be excited to contain coherent signal flux [19, 33]. Inspired by this finding, we propose a new gravitational wave detector design that includes two carriers at ω_1 and ω_2 and a beam at $\omega_L = (\omega_1 + \omega_2)/2$ serving as the heterodyne local oscillator. The three beams are evenly separated by RF, ω_m. This new design with heterodyne readout will lead to an identical quantum-limited sensitivity performance to that with homodyne readout and the same total arm power, *i.e.* the sum of the power of the two carriers circulating in the arm equals to the arm cavity power in the single carrier detector with homodyne readout.

Another highlight of the two-carrier detector with heterodyne readout is on the simpleness of the generation and application of quantum squeezing. Most gravitational-wave signals from compact binary system detected by ground-based detectors are within the audio band, from several Hz to several kHz. However, at audio frequencies, excess noises are significant due to the parasitic interferences from back-scattered light [34, 35] and noise coupling from control beams [36–41]. Good squeezing is easier to produce and to be observed at high frequencies in the MHz range where the classical noise of the laser is negligible. We will show that instead of audio-band squeezing [42, 43], high-frequency squeezing in boroadband two-mode quantum state is sufficient in our configuration. Our scheme naturally allows a measurement of low-frequency signals with high-frequency squeezing [44, 45].

Heterodyne readout and two-mode squeezing — In the two-photon formalism [46, 47], the photocurrent of a single sideband heterodyne readout is proportional to the combined quadrature [48]

$$\hat{Q}_\zeta = \mathbf{H}_\zeta \cdot \left[\hat{X}_1 \;\; \hat{Y}_1 \;\; \hat{X}_2 \;\; \hat{Y}_2\right]^{\mathrm{T}} , \tag{1}$$

with $\mathbf{H}_\zeta \equiv [\cos\zeta_1, \sin\zeta_1, \cos\zeta_2, \sin\zeta_2]$. Here $\hat{X}_j, \hat{Y}_j$ ($j = 1, 2$) represent the amplitude and phase quadrature of the sidebands near ω_1 and ω_2, respectively; ζ_j defines the measurement quadrature,

$$\zeta_1 = \phi_L - \phi_D \, , \zeta_2 = \phi_L + \phi_D \tag{2}$$

where ϕ_L is the local oscillator phase and is assumed to be $\pi/2$ in this work, ϕ_D is the demodulation phase. We normalise the shot noise spectral density for the vacuum state to be 1. In the two-mode quantum state, ω_1 and ω_2 are correlated [14, 41, 48, 49], of which the correlation is quantified by the covariance matrix,

$$\mathbb{V} = \begin{bmatrix} \alpha & 0 & \beta & 0 \\ 0 & \alpha & 0 & -\beta \\ \beta & 0 & \alpha & 0 \\ 0 & -\beta & 0 & \alpha \end{bmatrix} , \tag{3}$$

where $\alpha = \cosh 2r, \beta = \sinh 2r$ and r is the phase squeezing factor. The spectral density of the combined quadrature $\hat{Q}_\zeta$ in Eq. (1) is given by

$$\mathbf{H}_\zeta \mathbb{V} \mathbf{H}_\zeta^{\mathrm{T}} = 2\alpha \pm 2\beta = 2e^{\pm 2r} , \tag{4}$$

which is a natural result of the EPR entanglement between quadratures of the two modes [16, 50–52], as illustrated in Fig. 2.

Quantum noise of the detector — Inside the interferometer, the two sideband modes interact with the test mass through the radiation pressure force by beating with the two carriers. When the interferometer is tuned with equal power in the two carriers, the opto-mechanical factors describing the interaction of the modes with the test mass mirrors and their cross correlation are identical. They are equal to a half of the opto-mechanical factor $\mathcal{K}$ defined in Ref. [53]. Note here because ω_m is much smaller than ω_j, we neglect the effect of difference of wavelength of two carriers. The input-output transfer matrix $\mathbb{T}$ for the quadratures of these two modes and

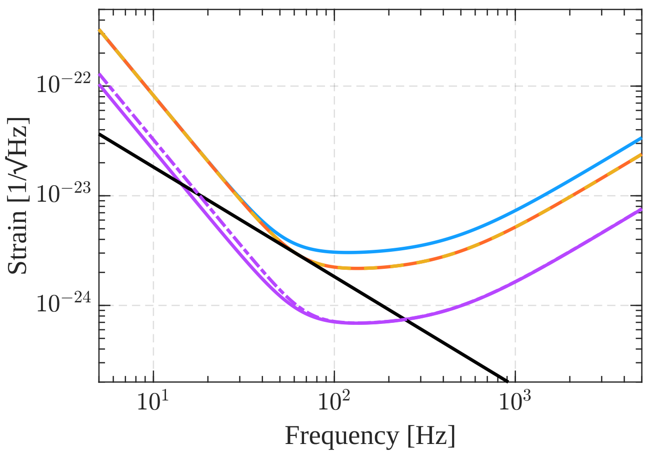

FIG. 3. Quantum-limited sensitivity of different configurations. The blue curve corresponds to the case of single carrier with heterodyne readout; the orange curve corresponds to the two-carrier detector, which perfectly overlaps with the yellow dash curve for homodyne readout; the purple solid curve is sensitivity of two-carrier detector with 10dB squeezing; the purple dot-dash curve corresponds to 15% power imbalanced between two carriers, *i.e.* $\eta = 0.575$. The balck curve is the Standard Quantum Limit. The parameters used in the two-carrier detector are the same as that of Advanced LIGO [11].

their response vector $\mathbf{R}$ of the interferometer to the gravitational wave strain can be derived as

$$\mathbb{T} = e^{2i\beta}\begin{bmatrix} 1 & 0 & 0 & 0 \\ -\mathcal{K}/2 & 1 & -\mathcal{K}/2 & 0 \\ 0 & 0 & 1 & 0 \\ -\mathcal{K}/2 & 0 & -\mathcal{K}/2 & 1 \end{bmatrix},\ \mathbf{R} = \frac{e^{i\beta}}{h_{\rm SQL}}\begin{bmatrix} 0 \\ \sqrt{\mathcal{K}} \\ 0 \\ \sqrt{\mathcal{K}} \end{bmatrix}. \quad (5)$$

Here $\beta = \text{atan}(\Omega/\gamma)$ is the phase of the sidebands at frequency Ω acquired reflecting off from the inteferometer with a bandwidth γ. The opto-mechanical factor is

$$\mathcal{K} = \frac{16\omega_0 P\gamma}{mcL\Omega^2(\gamma^2+\Omega^2)}\,, \quad (6)$$

where m is the mirror mass, P is the total circulating power in the arm cavity. The Standard Quantum Limit of the detector in strain is $h_{\rm SQL} = \sqrt{8\hbar/(m\Omega^2L^2)}$.

The low-frequency radiation pressure noise can be improved by using the frequency-dependent squeezing [53]. In the broadband detection mode, the same as the single-carrier detector, we only need one filter cavity for the two-carrier detector, as long as the free spectral range of the filter cavity is integer number of $2\omega_m$. The filter cavity provides a frequency dependent quadrature rotation θ_1, θ_2 for the two modes, which can be described by [54]

$$\mathbb{P}_\theta = \begin{bmatrix} \cos\theta_1 & -\sin\theta_1 & 0 & 0 \\ \sin\theta_1 & \cos\theta_1 & 0 & 0 \\ 0 & 0 & \cos\theta_2 & -\sin\theta_2 \\ 0 & 0 & \sin\theta_2 & \cos\theta_2 \end{bmatrix}. \quad (7)$$

The quantum noise spectral density of heterodyne readout, normalised to the strain response, is given by

$$S_{hh} = h_{\rm SQL}^2\frac{\mathbf{H}_\zeta\mathbb{T}\mathbb{P}_\theta\mathbb{V}\mathbb{P}_\theta^{\rm T}\mathbb{T}^\dagger\mathbf{H}_\zeta^{\rm T}}{|\mathbf{H}_\zeta\mathbf{R}|^2}\,. \quad (8)$$

When the frequency-dependent rotation angle satisfies

$$\theta_1 = \theta_2 = \text{atan}\,\mathcal{K}\,, \quad (9)$$

the noise spectrum reaches the minimal value

$$S_{hh}^{\rm min} = \frac{h_{\rm SQL}^2}{2}\frac{\mathcal{K}^2+1}{\mathcal{K}}e^{-2r}\,. \quad (10)$$

In Fig. 3, we plot the noise spectral densities for different configurations as a comparison. The two-carrier detector with heterodyne readout gives identical sensitivity to that of Advanced LIGO with homodyne readout. The figure also shows that the scheme is robust against a power imbalance between the two carriers: at 10 dB frequency-dependent squeezing, considering 15% strong power imbalanced between two carriers, it only results in a 20% worse sensitivity at low frequencies.

Criterias of macroscope lengths — One important difference between our proposed scheme and the single-carrier detector is that lengths between core optics need to be carefully set to defined absolute values to guarantee co-resonance of the respective optical fields. This introduces new requirements on the macroscopic lengths, in addition to the usual requirement for controlling the microscopic position of the optics via feedback.

To keep the carriers resonant and the local oscillator beam anti-resonant in the arm cavities, $2\omega_m$ shall be the odd times free spectral range of the arm cavity, $\frac{c}{2L}$. Another consideration is on the coupling between the symmetric and anti-symmetric ports for both the carriers and the local oscillator. The central Michelson can be treated as an effective mirror with the amplitude transmissivity, $t_{\rm MI} = A\sin\omega\Delta L/c$ and reflectivity $r_{\rm MI} = A\cos\omega\Delta L/c$, where ΔL is the Schnupp asymmetry [32]. For the local oscillator, $A = -1, \omega = \omega_m$, and for the carrier at ω_1/ω_2, $A = 1, \omega = 0/2\omega_m$. In order to eliminate the couplings, there should be $2\omega_m\Delta L/c = \pi$. The macroscopic round-trip length of the signal recycling cavity and power recycling cavity should be tuned to provide an integer number times 2π phase accumulation for all three fields. Therefore, in the signal recycling cavity, the signal (carrier) modes are anti-resonant, while the local oscillator beam is resonant. In the power recycling cavity, all three beam are on resonance. In Advanced LIGO, ω_m is around 45 MHz, ΔL needs to be around 1.667 m. Given the Advanced LIGO power and signal recycling mirror transmissivity, 0.03 and 0.325, the effective power transmissivity of local oscillator field from symmetric port to anti-symmetric port is 30%. Finally, to implement frequency-dependent squeezing, according to Eq. (9), the required rotations for two modes are identical, which is also the same as that in the single-carrier detector with homodyne readout. To use one filter cavity for two modes, we need the integer times free spectral range of filter cavity equals to $2\omega_m$, as mentioned earlier.

Conclusions and Discussions — We have shown the proposed two-carrier gravitational wave detector with heterodyne readout leads to an identical quantum-limited sensitivity to the homodyne readout. To implement frequency dependent squeezing, only one filter cavity is required, which is the same as the single-carrier detector with homodyne readout. Furthermore, the two-carrier detector also provides advantages for mitigating other noise contributions: (1) it enables squeezing enhanced measurements in the audio-band and below with high-frequency squeezing, which is immune to the low-frequency classical noise; (2) it allows us to operate the interferometer on the dark fringe without an additional local oscillator path and output mode cleaners that are essential to balanced homodyne readout scheme [48]. Compared with the single-carrier detector, there is added complexity related to the creation of two carriers on the input laser side. We also need a detailed study of the modulation scheme and technical-noise couplings, *e.g.* laser frequency noise coupling due to a larger Schnupp asymmetry, in order to eventually implement it.

As an outlook, we also want to highlight that the two-carrier detector is also compatible to general quantum nondemolition (QND) measurement schemes [55, 56], in contrast to the conventional heterodyne readout [23]. For example, similar to the implementation of frequency dependent squeezing, we can add a filter cavity at the output to realise frequency-dependent readout for back action evasion [53]. The resulting optimal sensitivity is

$$S_{hh}^{\rm opt} = \frac{h_{\rm SQL}^2}{2}\frac{1}{\mathcal{K}}e^{-2r}\,. \tag{11}$$

This saturates the fundamental quantum limit or the quantum Cramér-Rao bound [57–61].

Acknowledgements — We thank the support from simulation software, *Finesse*. T. Z., P.J, H. M., D. M. and A. F. acknowledge the support of the Institute for Gravitational Wave Astronomy at University of Birmingham. A. F. has been supported by a Royal Society Wolfson Fellowship which is jointly funded by the Royal Society and the Wolfson Foundation. H. M. is supported by UK STFC Ernest Rutherford Fellowship (Grant No. ST/M005844/11). S.W.B. acknowledges the supported by the National Science Foundation award PHY-1912536. This document was assigned the LIGO documnet control number LIGO-P2000260.

[1] B. Abbott, R. Abbott, T. Abbott, M. Abernathy, F. Acernese, K. Ackley, C. Adams, T. Adams, P. Addesso, R. Adhikari, *et al.* (LIGO Scientific Collaboration and Virgo Collaboration), Observation of gravitational waves from a binary black hole merger, Phys. Rev. Lett. **116**, 061102 (2016).

[2] B. Abbott, R. Abbott, T. Abbott, M. Abernathy, F. Acernese, K. Ackley, C. Adams, T. Adams, P. Addesso, R. Adhikari, *et al.* (LIGO Scientific Collaboration and Virgo Collaboration), Gw170817: Observation of gravitational waves from a binary neutron star inspiral, Phys. Rev. Lett. **119**, 161101 (2017).

[3] B. Abbott, R. Abbott, T. Abbott, M. Abernathy, F. Acernese, K. Ackley, C. Adams, T. Adams, P. Addesso, R. Adhikari, *et al.* (LIGO Scientific Collaboration and Virgo Collaboration), Gwtc-1: A gravitational-wave transient catalog of compact binary mergers observed by ligo and virgo during the first and second observing runs, Phys. Rev. X **9**, 031040 (2019).

[4] A. Buonanno and Y. Chen, Signal recycled laser-interferometer gravitational-wave detectors as optical springs, Phys. Rev. D **65**, 042001 (2002).

[5] A. Buonanno and Y. Chen, Scaling law in signal recycled laser-interferometer gravitational-wave detectors, Phys. Rev. D **67**, 062002 (2003).

[6] P. Fritschel, M. Evans, and V. Frolov, Balanced homodyne readout for quantum limited gravitational wave detectors, Opt. Express **22**, 4224 (2014).

[7] R. W. P. Drever, J. L. Hall, F. V. Kowalski, J. Hough, G. M. Ford, A. J. Munley, and H. Ward, Laser phase and frequency stabilization using an optical resonator, Applied Physics B **31**, 97 (1983).

[8] E. D. Black, An introduction to pound–drever–hall laser frequency stabilization, American Journal of Physics **69**, 79 (2001).

[9] R. Takahashi and the TAMA Collaboration, Status of TAMA300, Classical and Quantum Gravity **21**, S403 (2004).

[10] F. Acernese, P. Amico, M. Al-Shourbagy, S. Aoudia, S. Avino, D. Babusci, G. Ballardin, F. Barone, *et al.*, The status of VIRGO, Classical and Quantum Gravity **23**, S63 (2006).

[11] J. Aasi, B. P. Abbott, R. Abbott, T. Abbott, M. R. Abernathy, K. Ackley, C. Adams, T. Adams, P. Addesso, R. X. Adhikari, and L. S. Collaboration, Advanced LIGO, Classical and Quantum Gravity **32**, 074001 (2015).

[12] F. Acernese, M. Agathos, K. Agatsuma, D. Aisa, N. Allemandou, A. Allocca, J. Amarni, P. Astone, *et al.*, Advanced virgo: a second-generation interferometric gravitational wave detector, Classical and Quantum Gravity **32**, 024001 (2014).

[13] T. Akutsu, M. Ando, K. Arai, Y. Arai, S. Araki, A. Araya, and K. collaboration, Kagra: 2.5 generation interferometric gravitational wave detector, Nature Astronomy **3**, 35 (2019).

[14] J. Gea-Banacloche and G. Leuchs, Squeezed states for interferometric gravitational-wave detectors, Journal of Modern Optics **34**, 793 (1987).

[15] V. Chickarmane, S. V. Dhurandhar, T. C. Ralph, M. Gray, H.-A. Bachor, and D. E. McClelland, Squeezed light in a frontal-phase-modulated signal-recycled inter-

ferometer, Phys. Rev. A **57**, 3898 (1998).
[16] A. M. Marino, J. C. R. Stroud, V. Wong, R. S. Bennink, and R. W. Boyd, Bichromatic local oscillator for detection of two-mode squeezed states of light, J. Opt. Soc. Am. B **24**, 335 (2007).
[17] W. Li, X. Yu, and J. Zhang, Measurement of the squeezed vacuum state by a bichromatic local oscillator, Opt. Lett. **40**, 5299 (2015).
[18] S. Feng, D. He, and B. Xie, Quantum theory of phase-sensitive heterodyne detection, J. Opt. Soc. Am. B **33**, 1365 (2016).
[19] M. Collett, R. Loudon, and C. Gardiner, Quantum theory of optical homodyne and heterodyne detection, Journal of Modern Optics **34**, 881 (1987).
[20] S. D. Personick, B.s.t.j. brief: An image band interpretation of optical heterodyne noise, The Bell System Technical Journal **50**, 213 (1971).
[21] H. P. Yuen and V. W. S. Chan, Noise in homodyne and heterodyne detection, Opt. Lett. **8**, 177 (1983).
[22] C. M. Caves and P. D. Drummond, Quantum limits on bosonic communication rates, Rev. Mod. Phys. **66**, 481 (1994).
[23] A. Buonanno, Y. Chen, and N. Mavalvala, Quantum noise in laser-interferometer gravitational-wave detectors with a heterodyne readout scheme, Phys. Rev. D **67**, 122005 (2003).
[24] D. S. (for the LIGO Scientific Collaboration), Status of the LIGO detectors, Classical and Quantum Gravity **25**, 114041 (2008).
[25] F. Acernese, M. Alshourbagy, P. Amico, F. Antonucci, S. Aoudia, P. Astone, S. Avino, L. Baggio, *et al.*, Status of virgo, Classical and Quantum Gravity **25**, 114045 (2008).
[26] H. G. and, The status of GEO 600, Classical and Quantum Gravity **25**, 114043 (2008).
[27] S. Hild, H. Grote, J. Degallaix, S. Chelkowski, K. Danzmann, A. Freise, M. Hewitson, J. Hough, H. Lück, M. Prijatelj, K. A. Strain, J. R. Smith, and B. Willke, DC-readout of a signal-recycled gravitational wave detector, Classical and Quantum Gravity **26**, 055012 (2009).
[28] T. T. Fricke, N. D. Smith-Lefebvre, R. Abbott, R. Adhikari, K. L. Dooley, M. Evans, P. Fritschel, V. V. Frolov, K. Kawabe, J. S. Kissel, B. J. J. Slagmolen, and S. J. Waldman, DC readout experiment in enhanced LIGO, Classical and Quantum Gravity **29**, 065005 (2012).
[29] H. Yu, D. Martynov, S. Vitale, M. Evans, D. Shoemaker, B. Barr, G. Hammond, S. Hild, J. Hough, S. Huttner, S. Rowan, B. Sorazu, L. Carbone, A. Freise, C. Mow-Lowry, K. L. Dooley, P. Fulda, H. Grote, and D. Sigg, Prospects for detecting gravitational waves at 5 hz with ground-based detectors, Phys. Rev. Lett. **120**, 141102 (2018).
[30] S. Steinlechner, B. W. Barr, A. S. Bell, S. L. Danilishin, A. Gläfke, C. Gräf, J.-S. Hennig, E. A. Houston, S. H. Huttner, S. S. Leavey, D. Pascucci, B. Sorazu, A. Spencer, K. A. Strain, J. Wright, and S. Hild, Local-oscillator noise coupling in balanced homodyne readout for advanced gravitational wave detectors, Phys. Rev. D **92**, 072009 (2015).
[31] M. A. Arain and G. Mueller, Design of the advanced ligo recycling cavities, Optics Express **16**, 10018 (2008).
[32] K. Izumi and D. Sigg, Advanced LIGO: length sensing and control in a dual recycled interferometric gravitational wave antenna, Classical and Quantum Gravity **34**, 015001 (2016).
[33] H. Fan, D. He, and S. Feng, Experimental study of a phase-sensitive heterodyne detector, J. Opt. Soc. Am. B **32**, 2172 (2015).
[34] H. Vahlbruch, S. Chelkowski, K. Danzmann, and R. Schnabel, Quantum engineering of squeezed states for quantum communication and metrology, New Journal of Physics **9**, 371 (2007).
[35] S. S. Y. Chua, S. Dwyer, L. Barsotti, D. Sigg, R. M. S. Schofield, V. V. Frolov, K. Kawabe, M. Evans, G. D. Meadors, M. Factourovich, R. Gustafson, N. Smith-Lefebvre, C. Vorvick, M. Landry, A. Khalaidovski, M. S. Stefszky, C. M. Mow-Lowry, B. C. Buchler, D. A. Shaddock, P. K. Lam, R. Schnabel, N. Mavalvala, and D. E. McClelland, Impact of backscattered light in a squeezing-enhanced interferometric gravitational-wave detector, Classical and Quantum Gravity **31**, 035017 (2014).
[36] W. P. Bowen, R. Schnabel, N. Treps, H.-A. Bachor, and P. K. Lam, Recovery of continuous wave squeezing at low frequencies, Journal of Optics B: Quantum and Semiclassical Optics **4**, 421 (2002).
[37] K. McKenzie, E. E. Mikhailov, K. Goda, P. K. Lam, N. Grosse, M. B. Gray, N. Mavalvala, and D. E. McClelland, Quantum noise locking, Journal of Optics B: Quantum and Semiclassical Optics **7**, S421 (2005).
[38] H. Vahlbruch, S. Chelkowski, B. Hage, A. Franzen, K. Danzmann, and R. Schnabel, Squeezed-field injection for gravitational wave interferometers, Classical and Quantum Gravity **23**, S251 (2006).
[39] R. Schnabel, J. Harms, K. A. Strain, and K. Danzmann, Squeezed light for the interferometric detection of high-frequency gravitational waves, Classical and Quantum Gravity **21**, S1045 (2004).
[40] K. McKenzie, N. Grosse, W. P. Bowen, S. E. Whitcomb, M. B. Gray, D. E. McClelland, and P. K. Lam, Squeezing in the audio gravitational-wave detection band, Phys. Rev. Lett. **93**, 161105 (2004).
[41] R. Schnabel, Squeezed states of light and their applications in laser interferometers, Physics Reports **684**, 1 (2017), squeezed states of light and their applications in laser interferometers.
[42] J. Abadie, B. P. Abbott, R. Abbott, T. D. Abbott, *et al.* (LIGO Scientific Collaboration), A gravitational wave observatory operating beyond the quantum shot-noise limit, Nature Physics **7**, 962 (2011).
[43] J. Aasi, J. Abadie, B. P. Abbott, R. Abbott, T. D. Abbott, M. R. Abernathy, *et al.* (LIGO Scientific Collaboration), Enhanced sensitivity of the ligo gravitational wave detector by using squeezed states of light, Nature Photonics **7**, 613 (2013).
[44] Z. Zhai and J. Gao, Low-frequency phase measurement with high-frequency squeezing, Opt. Express **20**, 18173 (2012).
[45] W. Li, Y. Jin, X. Yu, and J. Zhang, Enhanced detection of a low-frequency signal by using broad squeezed light and a bichromatic local oscillator, Phys. Rev. A **96**, 023808 (2017).
[46] C. M. Caves and B. L. Schumaker, New formalism for two-photon quantum optics. i. quadrature phases and squeezed states, Phys. Rev. A **31**, 3068 (1985).
[47] B. L. Schumaker and C. M. Caves, New formalism for two-photon quantum optics. ii. mathematical foundation and compact notation, Phys. Rev. A **31**, 3093 (1985).

[48] T. Zhang, D. Martynov, A. Freise, and H. Miao, Quantum squeezing schemes for heterodyne readout, arXiv preprint arXiv:2004.10503 (2020).

[49] J. Zhang, Einstein-podolsky-rosen sideband entanglement in broadband squeezed light, Phys. Rev. A **67**, 054302 (2003).

[50] Y. Ma, H. Miao, B. H. Pang, M. Evans, C. Zhao, J. Harms, R. Schnabel, and Y. Chen, Proposal for gravitational-wave detection beyond the standard quantum limit through epr entanglement, Nature Physics **13**, 776 EP (2017).

[51] S. L. Danilishin, F. Y. Khalili, and H. Miao, Advanced quantum techniques for future gravitational-wave detectors, Living Reviews in Relativity **22**, 2 (2019).

[52] J. Südbeck, S. Steinlechner, M. Korobko, and R. Schnabel, Demonstration of interferometer enhancement through einstein–podolsky–rosen entanglement, Nature Photonics **14**, 240 (2020).

[53] H. J. Kimble, Y. Levin, A. B. Matsko, K. S. Thorne, and S. P. Vyatchanin, Conversion of conventional gravitational-wave interferometers into quantum nondemolition interferometers by modifying their input and/or output optics, Phys. Rev. D **65**, 022002 (2001).

[54] S. L. Danilishin and F. Y. Khalili, Quantum measurement theory in gravitational-wave detectors, Living Reviews in Relativity **15** (2012).

[55] V. B. Braginsky, Y. I. Vorontsov, and K. S. Thorne, Quantum nondemolition measurements, Science **209**, 547 (1980).

[56] Y. Chen, S. L. Danilishin, F. Y. Khalili, and H. Müller-Ebhardt, Qnd measurements for future gravitational-wave detectors, General Relativity and Gravitation **43**, 671 (2011).

[57] C. Helstrom, Minimum mean-squared error of estimates in quantum statistics, Physics Letters A **25**, 101 (1967).

[58] A. S. Holevo, *Probabilistic and statistical aspects of quantum theory*, Vol. 1 (Springer Science & Business Media, 2011).

[59] V. B. Braginsky, M. L. Gorodetsky, F. Y. Khalili, and K. S. Thorne, Energetic quantum limit in large-scale interferometers, AIP Conference Proceedings **523**, 180 (2000).

[60] M. Tsang, H. M. Wiseman, and C. M. Caves, Fundamental quantum limit to waveform estimation, Phys. Rev. Lett. **106**, 090401 (2011).

[61] H. Miao, R. X. Adhikari, Y. Ma, B. Pang, and Y. Chen, Towards the fundamental quantum limit of linear measurements of classical signals, Phys. Rev. Lett. **119**, 050801 (2017).